



Laser speckle contrast imaging and quantitative fluorescence angiography for perfusion assessment

Jonas Hedelund Rønn¹ · Nikolaj Nerup¹ · Rune Broni Strandby¹ · Morten Bo Søndergaard Svendsen² · Rikard Ambrus¹ · Lars Bo Svendsen¹ · Michael Patrick Achiam¹

Received: 4 January 2019 / Accepted: 17 April 2019 / Published online: 4 May 2019
© Springer-Verlag GmbH Germany, part of Springer Nature 2019

Abstract

Purpose Indocyanine green fluorescence angiography (ICG-FA) is an established technique for assessment of intestinal perfusion during gastrointestinal surgery, whereas quantitative ICG-FA (q-ICG) and laser speckle contrast imaging (LSCI) are relatively unproven. The study aimed to investigate whether the techniques could be applied interchangeably for perfusion assessment.

Methods Nineteen pigs underwent laparotomy, two minor resections of the small bowel, and anastomoses. Additionally, seven pigs had parts of their stomach and small intestine de-vascularized. Data was also collected from an in vivo model (inferior caval vein measurements in two additional pigs) and an ex vivo flow model, allowing for standardization of experimental flow, distance, and angulation. Q-ICG and LSCI were performed, so that regions of interest were matched between the two modalities in the analyses, ensuring coverage of the same tissue.

Results The overall correlation of q-ICG and LSCI evaluated in the porcine model was modest ($\rho = 0.45, p < 0.001$), but high in tissue with low perfusion ($\rho = 0.74, p < 0.001$).

Flux values obtained by LSCI from the ex vivo flow model revealed a decreasing flux with linearly increasing distance as well as angulation to the model. The Q-ICG perfusion values obtained varied slightly with increasing distance as well as angulation to the model.

Conclusions Q-ICG and LSCI cannot be used interchangeably but may supplement each other. LSCI is profoundly affected by angulation and distance. In comparison, q-ICG is minimally affected by changing experimental conditions and is more readily applicable in minimally invasive surgery.

Keywords Perfusion imaging · Perfusion assessment · Fluorescence angiography · Laser speckle contrast imaging · Indocyanine green · Image-guided surgery

Introduction

Maintained perfusion of tissue is an important factor in sufficient healing of wounds and anastomoses [1], as poor

anastomotic perfusion is believed to be associated with anastomotic leakage (AL) [2, 3]. AL is a relatively common and feared complication, as it leads to a higher risk of local recurrence in oncologic surgery as well as increased short- and long-term morbidity and mortality [1, 2, 4–9].

Traditionally, tissue perfusion and subsequent gastrointestinal anastomotic viability have been assessed intraoperatively based on pulsation in the mesentery, coloration of tissue, and bleeding from resection lines. These clinical tools are, however, limited when minimally invasive techniques are utilized. Furthermore, this surgeon-based assessment has been proven to be of poor relation to preventing anastomotic leakage [7].

Indocyanine green fluorescence angiography (ICG-FA) and laser speckle contrast imaging (LSCI) are modalities used to visualize blood flow in tissue [10–12]. Historically, the modalities have been used in neurosurgery [13, 14], plastic surgery [15], ophthalmology [10, 11], and recently in

Jonas Hedelund Rønn and Nikolaj Nerup have contributed equally to the work, and share first author ship

✉ Nikolaj Nerup
nikolajnerup@gmail.com

¹ Department of Surgical Gastroenterology, Copenhagen University Hospital Rigshospitalet, Blegdamsvej 9, 2100 Copenhagen, Denmark

² Copenhagen Academy for Medical Education and Simulation, Center for Human Resources, Capital Region of Denmark, Rigshospitalet, Copenhagen, Denmark

gastrointestinal surgery [16]. ICG-FA relies on the injection of indocyanine green (ICG), a non-toxic water-soluble tricarboyanine dye, which binds to lipoproteins, and it is solely metabolized by the liver and excreted unchanged in the bile [17]. The fluorescent spectrum of ICG is in the range of near-infrared light and can be captured by a specialized camera after illumination of the tissue of interest (Figs. 1 and 2) [16]. Because the plasma disappearance rate of the ICG is high, deviations in the fluorescence signal can be taken to represent tissue perfusion. However, since most studies using ICG-FA are based on a visual assessment of the fluorescent image captured by the camera, the output is limited to a binary rating, perfused or non-perfused tissue [18]. Therefore, an algorithm to quantify the ICG-FA signal (q-ICG) has been developed and validated, advancing an objective evaluation of tissue perfusion [19]. Others have previously presented similar methods for quantification [20–22].

LSCI is based on the laser speckle pattern that arises when laser light illuminates a surface. The pattern is formed when

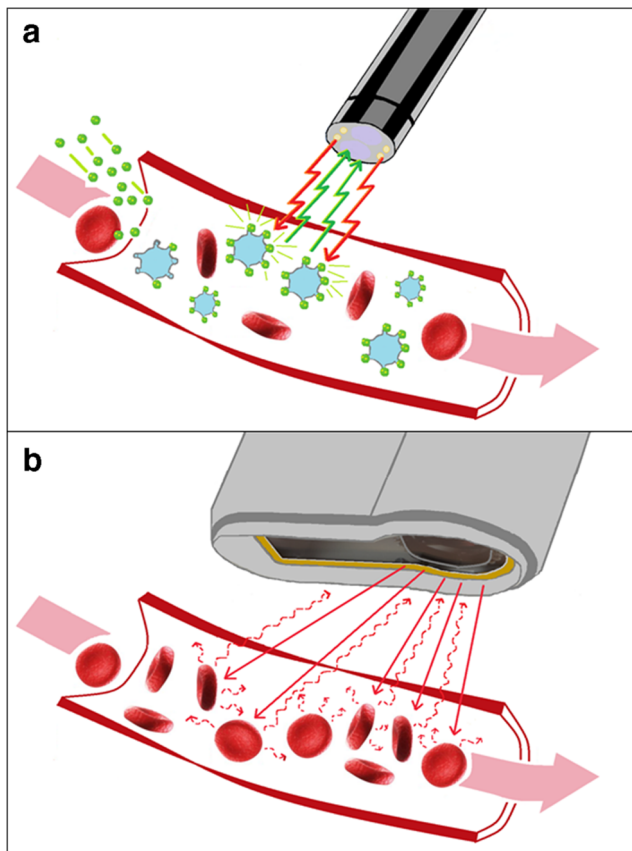


Fig. 1 Schematic drawing of the perfusion imaging techniques. **a** ICG-FA. Injected ICG binds to plasma proteins and fluoresces when illuminated with near-infrared light. The rate of fluorescence intensity over time is correlated linearly to microvascular flow. **b** LSCI. When laser light illuminates a surface a laser speckle pattern arises when scattered light creates an interference effect due to the irregularities of the structure. Movement of particles changes the scatter, and this can be extrapolated to laser speckle perfusion units

scattered light creates an interference effect due to the irregularities of the structure. If the object is moved or contains moving particles (e.g., blood cells), the interfering beam changes and produces a dynamic speckle pattern. Depending on the movements, the speckle pattern imaged differs over the finite exposure time of the camera and becomes more blurred with increasing movement. The level of blurring is quantified by a term called speckle contrast K , defined as

$$K = \frac{\sigma_i}{\langle I \rangle}$$

Here, σ_i is the standard deviation of the intensity and $\langle I \rangle$ is the mean of the pixel intensity [23, 10].

The speckle contrast is inversely related to the flow velocity. With higher flow velocity blurring increases and the standard deviation of the intensity decreases. Consequently, a lower speckle contrast is obtained. Conversely, with no flow blurring will decrease and the standard deviation increase, providing a larger speckle contrast. With a camera, the speckle contrast pattern can be analyzed and visualized, when a stack of the raw speckle images is processed to form an image, and fluctuations in the speckle contrast pattern are visualized as changes in the perfusion [24, 25] (Figs. 1 and 2).

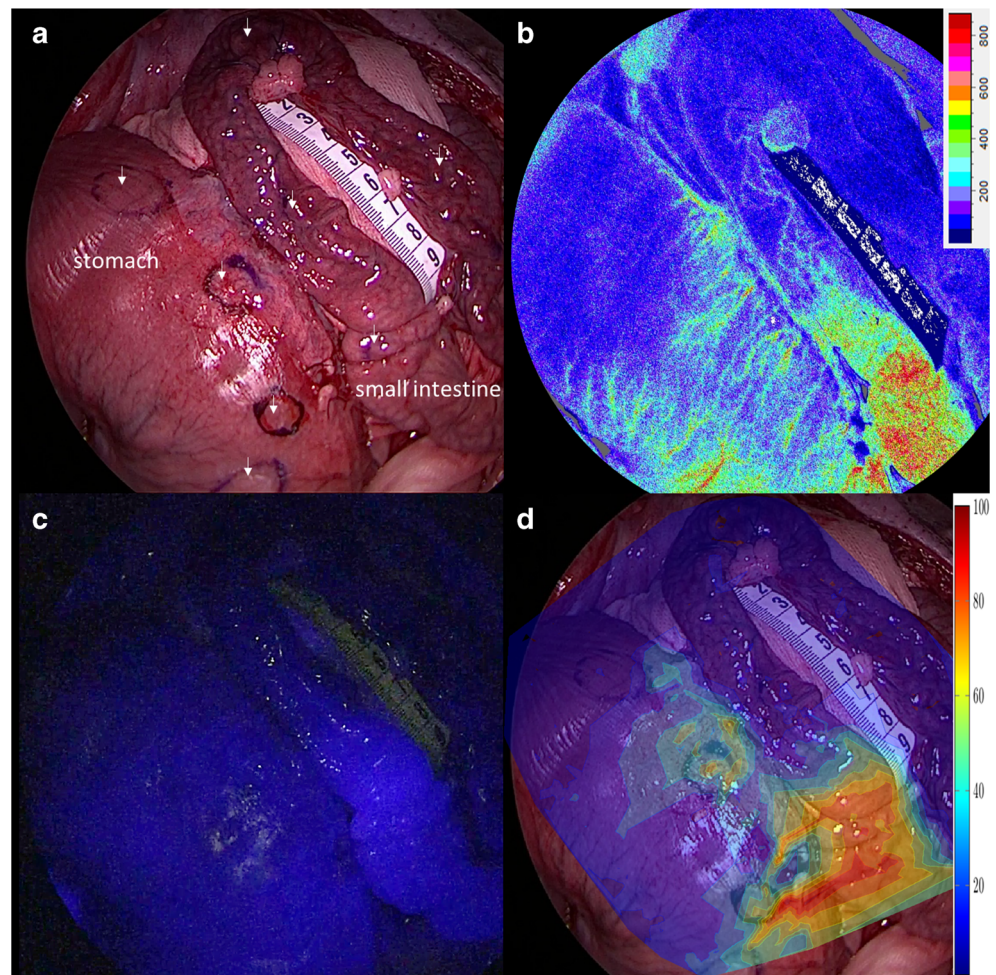
LSCI does not measure absolute flow, but an arbitrary unit is reported—laser speckle perfusion units (LSPU) [26]. However, both modalities have the advantages of being non-touch and can be applied in an easy, fast, and safe way [19, 26]. Since both modalities assess tissue perfusion, they should be coherent. While ICG-FA has been tested in gastrointestinal surgery, LSCI is relatively unproven in clinical settings. However, LSCI possesses some inherent advantages such as continuous evaluation of tissue perfusion and does not rely on contrast agents. So far, LSCI is not applicable for laparoscopic or robot-assisted surgical procedures challenging the clinical utility in a minimally invasive setting. It remains to be determined whether the modalities concur for evaluation of tissue perfusion, and how and to which extent LSCI and q-ICG are affected by changes in distance and the angle between the tissue and the measurement device. Advantages and limitations of the two modalities are thus essential to address.

This study aimed to explore whether LSCI may be used interchangeably, or complimentary, with q-ICG for assessment of gastrointestinal perfusion.

Material and methods

The study was based on data extracted from measurements in a porcine model and an ex vivo flow model. The projects were performed with the ambient light turned off unless otherwise is specified.

Fig. 2 Illustration of the de-vascularized stomach and small intestine. **a** White light, arrows indicate tissue lactate measurement. **b** LSCI image, color coding represents a snapshot of the flux (LSPU). **c** Snapshot of the ICG-FA. **d** Example of quantitative analysis of ICG-FA with color coding representing relative perfusion



All q-ICG measurements were performed using a laparoscope (ICG Hopkins® telescope 30°, Karl Storz GmbH and Co., KG, Tuttlingen, Germany) mounted on a stand to ensure standardization of the distance to the target surface, and to reduce motion artifacts. The scope was installed at 15 cm from the target at an angle of 45° to the surface unless otherwise is specified. The scope was connected to a camera system (IMAGE1, Karl Storz GmbH and Co., KG, Tuttlingen, Germany) and a light source (D-Light P, Karl Storz GmbH and Co., KG, Tuttlingen, Germany) supplying excitatory light for the ICG. Recordings of the angiographies were analyzed according to the method of q-ICG as described previously [19].

All LSCI measurements were performed using LSCI system with a wavelength of 785 nm (MoorFLPI, Moor Instruments Ltd., Axminster, UK). The device was mounted on a flexible arm allowing re-adjustments to standardize height and to reduce motion artifacts. The LSCI camera was placed approximately 25 cm above the target tissue as secured by the intersection of the aiming laser points according to the manufacturer's recommendation. The LSCI camera was placed perpendicular to the target surface unless otherwise is

specified and was set at high spatial resolution/low sampling rate (one frame per second) [26]. The extraction and analysis of data from the LSCI device were performed as described previously [26].

Regions of interest (ROIs) were matched for both LSCI and q-ICG allowing for a comparison of data collected from the same physical area.

Animals

The Danish Animal Experimentation Inspectorate approved the animal studies (#2016-15-0201-01015), and the studies were performed in accordance with the European Union legislation on animal experimentation, and the ARRIVE Guidelines [27]. Nineteen female pigs (Danish Landrace) with a mean weight of 35.9 kg (\pm 1.5 kg) were acclimatized 2 weeks before the start of the study (Department of Experimental Medicine, University of Copenhagen, Copenhagen) at standardized room temperatures, humidity, and light-dark hour cycles. On the morning of the procedure, the pigs were sedated by an intramuscular injection of Zoletil vet-mixture® (5 mg/kg) followed by intubation and induction of general

anesthesia (Propofol and Fentanyl, 15 mg/kg/h and 0.1 mg/kg/h, respectively). Ventilation was by a mixture of oxygen and atmospheric air aiming to maintain pO_2 and pCO_2 at 11–15 kPa and 4.5–6.5 kPa, respectively. The pigs underwent two laparotomies via a midline incision on day 1 and day 5. On day 1, two bowel segments of 5 cm each were resected followed by the establishment of two end-to-end anastomoses. ROIs in proximity to the anastomoses were marked followed by LSCI and q-ICG measurements. On day 5, all pigs underwent another laparotomy and measurements were repeated as described.

Additionally, in seven female pigs (Danish Landrace) following the same protocol as above, a segment of the small intestine was de-vascularized, and the blood supply to the stomach was ligated leaving only one third of the gastroepiploic artery and the right gastric artery. ROIs were marked along the intestine and the greater curvature of the stomach from healthy to the de-vascularized regions (Fig. 2). As local tissue lactate is considered an end-product of energy metabolism, we considered elevated lactates as a biomarker of tissue ischemia. After 30 min, local tissue lactate was measured using a handheld monitoring system (EDGE, Arctic Medical Ltd., Folkestone, UK) [28] and the perfusion was evaluated by LSCI and by q-ICG. For q-ICG measurements, a bolus of ICG (0.25 mg/kg; Verdye, Diagnostic Green GmbH, Aschheim-Dornach, Germany) was injected in the catheter of the ear vein followed by a saline flush (5 ml).

For analysis based on relative values, eight ROIs were chosen along the intestine and the greater curvature of the stomach from healthy to de-vascularized regions. The values of de-vascularized ROIs were compared with a reference value obtained from a mean of ROIs in the healthy region of the organ.

Investigation of physical properties

In two pigs following the same protocol as described above, the inferior caval vein (ICV) was exposed, as it represented a region of tissue with fast wash-in and wash-out of ICG. Thus, allowing for successive measurements with varying distance and angulation. For repeated q-ICG measurements boli of ICG (0.1 mg/kg) were injected. Due to the physical size and the configuration of the LSCI-system, LSCI recordings of the ICV were not possible. Instead, LSCI was evaluated in an ex vivo flow model established by a plastic tube (standard suction tube) mounted on a peristaltic pump (Minipuls 3 peristaltic pump; Gilson Inc., Middleton, WI, USA) perfused by heparinized (500 IU) porcine blood. Measurements were applied on the surface of the plastic tube and flushed with heparinized saline before the start of perfusion. The pump was set at 30 rpm corresponding to a flow of 9.5 ml/min, and a velocity of 24.7 cm/min.

The effect of distance to the target surface

The LSCI camera was placed 2 cm above the ex vivo model, and the blood flow was recorded for 30 s. Then, the LSCI camera was re-adjusted to 5 cm above the model, and the measurements were repeated. After that, measurements were repeated by 5-cm increments until 25 cm above the model. In a similar setup, q-ICG measurements were performed on the ICV, introducing an ICG-bolus before each measurement.

The effect of angulation between the surface and measurement device

The LSCI camera was placed pointing downward perpendicular to the plane of the model (0° angle), as per manufacturer instruction, and a video was recorded for 30 s. Then, the LSCI camera was tilted 10° , and the camera was refocused before measurements were repeated. The measurements were repeated by 10° increments until 80° tilt. A similar procedure was performed on the ICV as described using q-ICG. The ICG-laparoscope was installed at a 45° angle to the tissue surface (standard), in addition to the 30° angulation of the camera, resulting in a 15° angulation toward the tissue. Angles from 5° to 45° angulation to the tissue were investigated in 10° increments.

Statistics

Statistical calculations and graphs were performed by SPSS statistics (v22, IBM, Chicago, IL, USA) and GraphPad Prism (v8, GraphPad Software, San Diego, CA, USA).

Distribution of data was visually assessed by histograms and QQ plots. For correlation analysis, Spearman's rank correlation coefficient, rho, with 95% confidence interval (CI) was calculated due to one or both variables being skewed in histograms and QQ plots. Correlation coefficients of 0.00–0.30 were considered negligible, 0.30–0.50 low, 0.50–0.70 moderate, 0.70–0.90 high, and 0.90–1.00 very high [29]. Comparisons of correlation coefficients were done according to the Steiger method assisted by an online tool [30, 31]. The p values < 0.05 were considered significant.

Results

Correlation analyses of LSCI and q-ICG

Comparing all LSCI and q-ICG measurements showed a significant but low correlation between the two modalities $\rho = 0.448$ (95% CI 0.410, 0.484), $p < 0.001$, 1914 ROIs, $n = 26$ pigs.

When LSCI and q-ICG measurements were compared according to organ site, the correlations were found to be similar for the stomach and the small intestine (stomach: $\rho = 0.429$ (95% CI 0.339, 0.512), $p < 0.001$; 361 ROIs and small intestine: $\rho = 0.445$ (95% CI 0.401, 0.486), $p < 0.001$; 1454 ROIs, both $n = 26$ pigs). The correlation coefficients were not significantly different ($p = 0.74$).

LSCI and q-ICG measurements on the small intestines were compared according to de-vascularization vs. normoperfused. The correlation was found to be high in the de-vascularized subset ($\rho = 0.737$ (95% CI 0.695, 0.772), $p < 0.001$; 582 ROIs, $n = 7$ pigs) and was low for the normoperfused subset ($\rho = 0.414$ (95% CI 0.357, 0.470), $p < 0.001$; 872 ROIs, $n = 19$ pigs) (Fig. 3). When q-ICG and LSCI, in a subset, was compared based on percentages of the baseline values from normoperfused tissue, better correlations were found when compared with raw data from the normoperfused subset (stomach: $\rho = 0.549$ (95% CI 0.385, 0.680), $p < 0.001$; 88 ROIs, $n = 13$ pigs and small intestine: $\rho = 0.672$ (95% CI 0.533, 0.776) $p < 0.001$; 88 ROIs, $n = 13$ pigs) (Fig. 4).

LSCI and q-ICG were also evaluated in comparison with tissue lactate ($n = 7$ pigs). A significant negative correlation was found between both LSCI and q-ICG and tissue lactate; i.e., at increasing tissue lactate levels both modalities registered a decreased perfusion (q-ICG: $\rho = -0.771$ (-0.887, -0.566), $p < 0.001$, 31 ROIs and LSCI: $\rho = -0.840$ (-0.922, -0.686), $p < 0.001$, 31 ROIs) (Fig. 5). The correlation coefficients were not significantly different ($p = 0.32$).

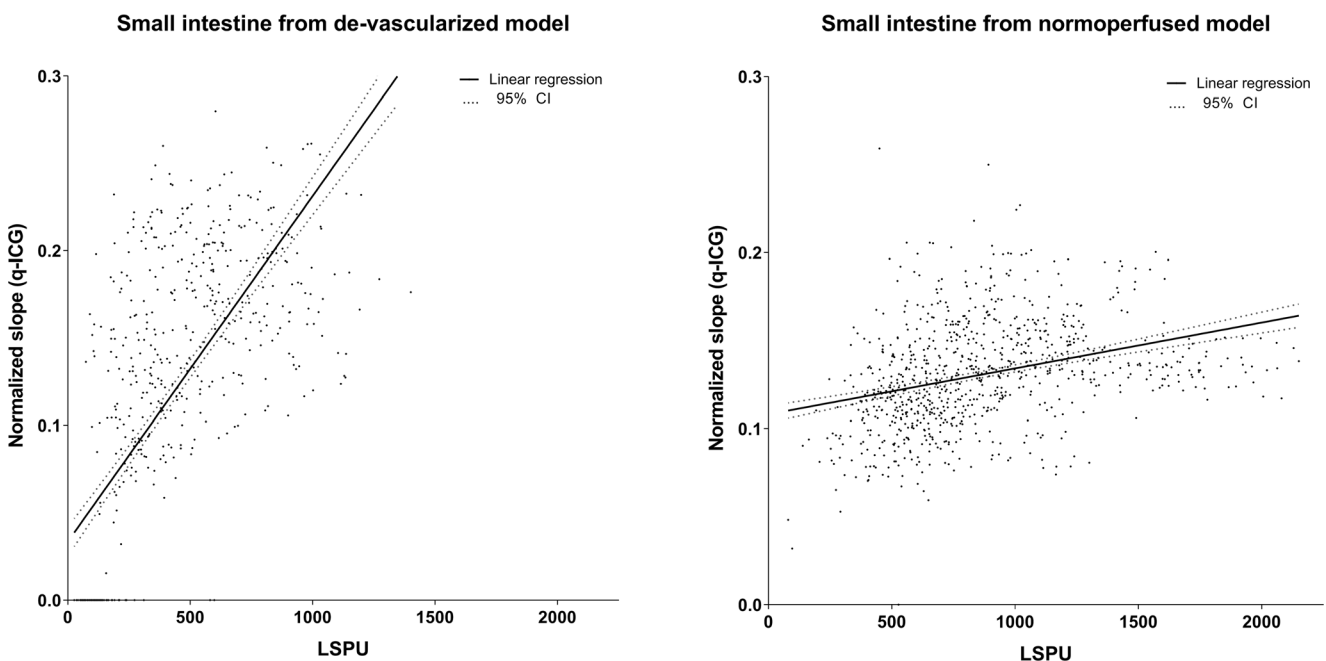


Fig. 3 Scatterplot of data obtained from porcine models by LSCI and q-ICG. Linear regression lines with 95% CI are shown. Left: de-vascularization (582 ROIs, $n = 7$ pigs), Spearman's $\rho = 0.74$ (95% CI 0.70, 0.77; $p < 0.001$). Right: normoperfusion (872 ROIs, $n = 19$ pigs),

Investigation of physical properties

Effect of angulation With increasing angle between the LSCI camera and the flow model, a linear decrease in LSPU was found, slope -13.65 , intercept 925.3 , $R^2 = 0.97$, $p < 0.001$, five ROIs/measurement. At an angulation of 60° and higher, the LSCI system was no longer able to obtain recordings. In contrast, the q-ICG assessed perfusion increased only slightly in response to angulation; pig 1: slope 0.0009786 , intercept 0.04589 , $R^2 = 0.50$, $p = 0.0033$; pig 2: slope 0.0003065 , intercept 0.08765 , $R^2 = 0.12$, $p = 0.21$ (three ROIs/measurement, $n = 2$ pigs) (Fig. 6).

Effect of distance By increasing distance from the LSCI camera to the flow model a decrease in the LSPU was found, slope -61.10 , intercept 2486 , $R^2 = 0.88$, $p < 0.001$, five ROIs/measurement. Similarly, to the effect of angulation, slightly lower perfusion measures were detected by q-ICG when the distance from the scope to the tissue increased; pig 1: slope $0.0002057x + 0.06027$, $R^2 = 0.023$, $p = 0.55$; pig 2: slope -0.0009610 , intercept 0.09969 , $R^2 = 0.48$, $p = 0.0013$ (three ROIs/measurement, $n = 2$ pigs) (Fig. 6).

Discussion

Based on data from the porcine models, the overall correlation between LSCI and q-ICG was low ($\rho = 0.45$). We found no significant difference in organ-specific correlations, yet, the

Spearman's $\rho = 0.41$ (95% CI 0.36, 0.47; $p < 0.001$). Normalized slope calculated as $(\Delta\text{fluorescence}/\Delta\text{time})/(\text{max fluorescence} - \text{baseline fluorescence})$. LSCI laser speckle contrast imaging, q-ICG quantitative indocyanine green, LSPU laser speckle perfusion units

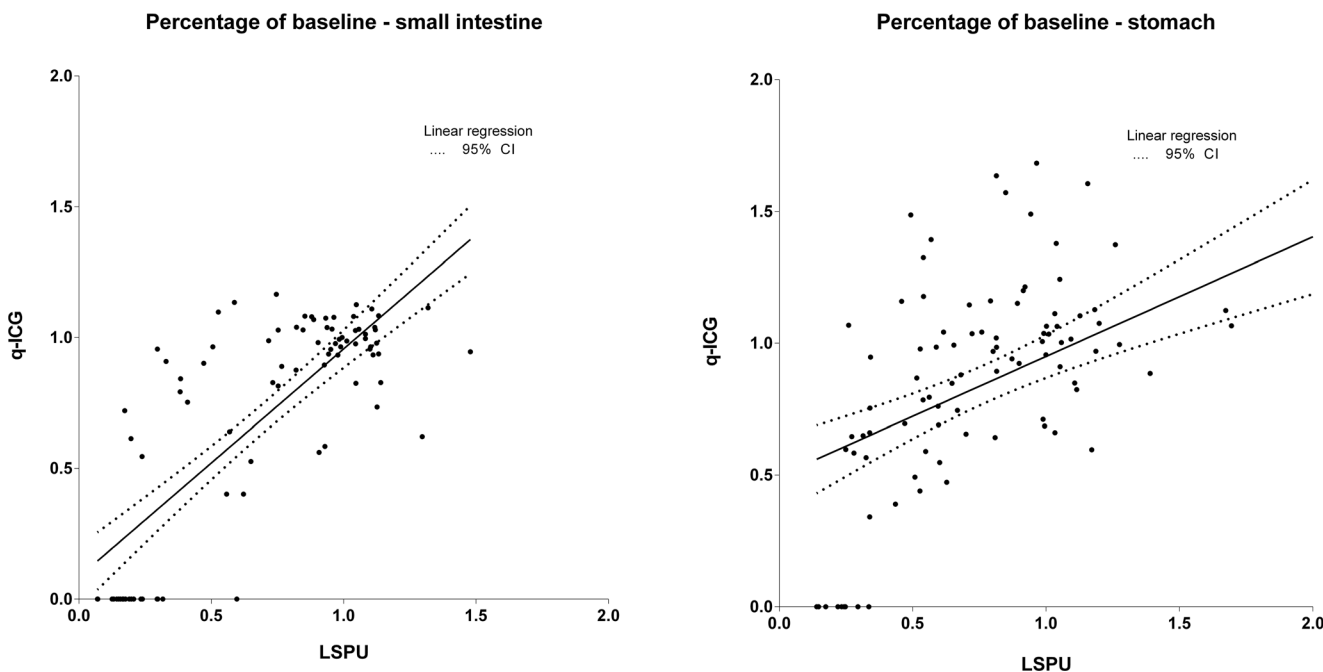


Fig. 4 Scatterplot of data obtained from porcine models (88 ROIs, $n = 13$ pigs) by LSCI and q-ICG illustrated as relative values (percentages of normoperfused tissue). Linear regression lines with 95% CI are shown. Left: Spearman’s rho = 0.67 (95% CI 0.53, 0.78; $p < 0.001$). Right:

Spearman’s rho = 0.55 (95% CI 0.39, 0.68; $p < 0.001$). Normalized slope calculated as $(\Delta\text{fluorescence}/\Delta\text{time})/(\text{max fluorescence} - \text{baseline fluorescence})$. LSCI laser speckle contrast imaging, q-ICG quantitative indocyanine green, LSPU laser speckle perfusion units

correlation between the two modalities was stronger in low perfused tissues compared with normally perfused tissue (rho = 0.74 for lowest de-vascularized small intestine vs. rho = 0.41 for non-de-vascularized small intestine). When LSCI

and q-ICG were compared with tissue lactates indicative of ischemia, the correlations were high for both LSCI and q-ICG (q-ICG: rho = -0.771, $p < 0.001$, and LSCI: rho = -0.840, $p < 0.001$).

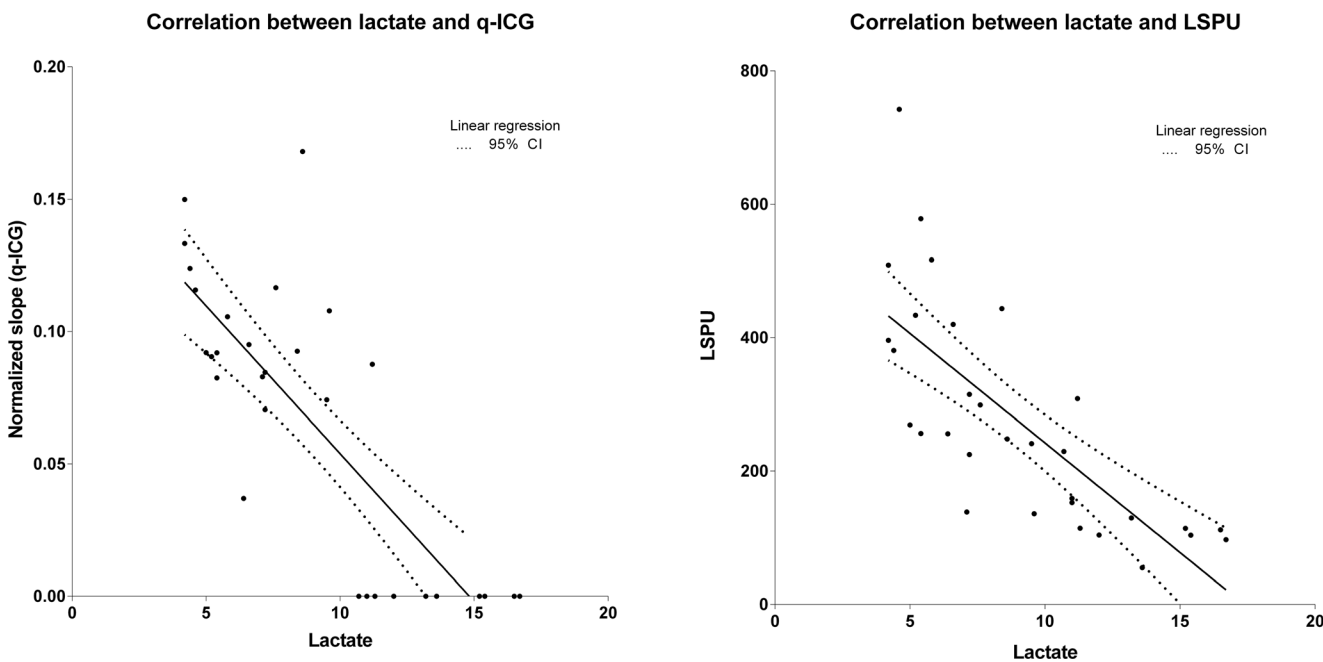


Fig. 5 Scatterplot of tissue lactate vs. normalized slope (q-ICG) (left) and lactate vs. LSPU (right) in de-vascularized bowel and stomach of $n = 7$ pigs, 88 ROIs. Left: Spearman’s rho = -0.77 (95% CI -0.89, -0.57; $p < 0.001$). Right: Spearman’s rho = -0.84 (95% CI -0.922, 0.686;

$p < 0.001$). Normalized slope calculated as $(\Delta\text{fluorescence}/\Delta\text{time})/(\text{max fluorescence} - \text{baseline fluorescence})$. q-ICG quantitative indocyanine green, LSPU laser speckle perfusion units

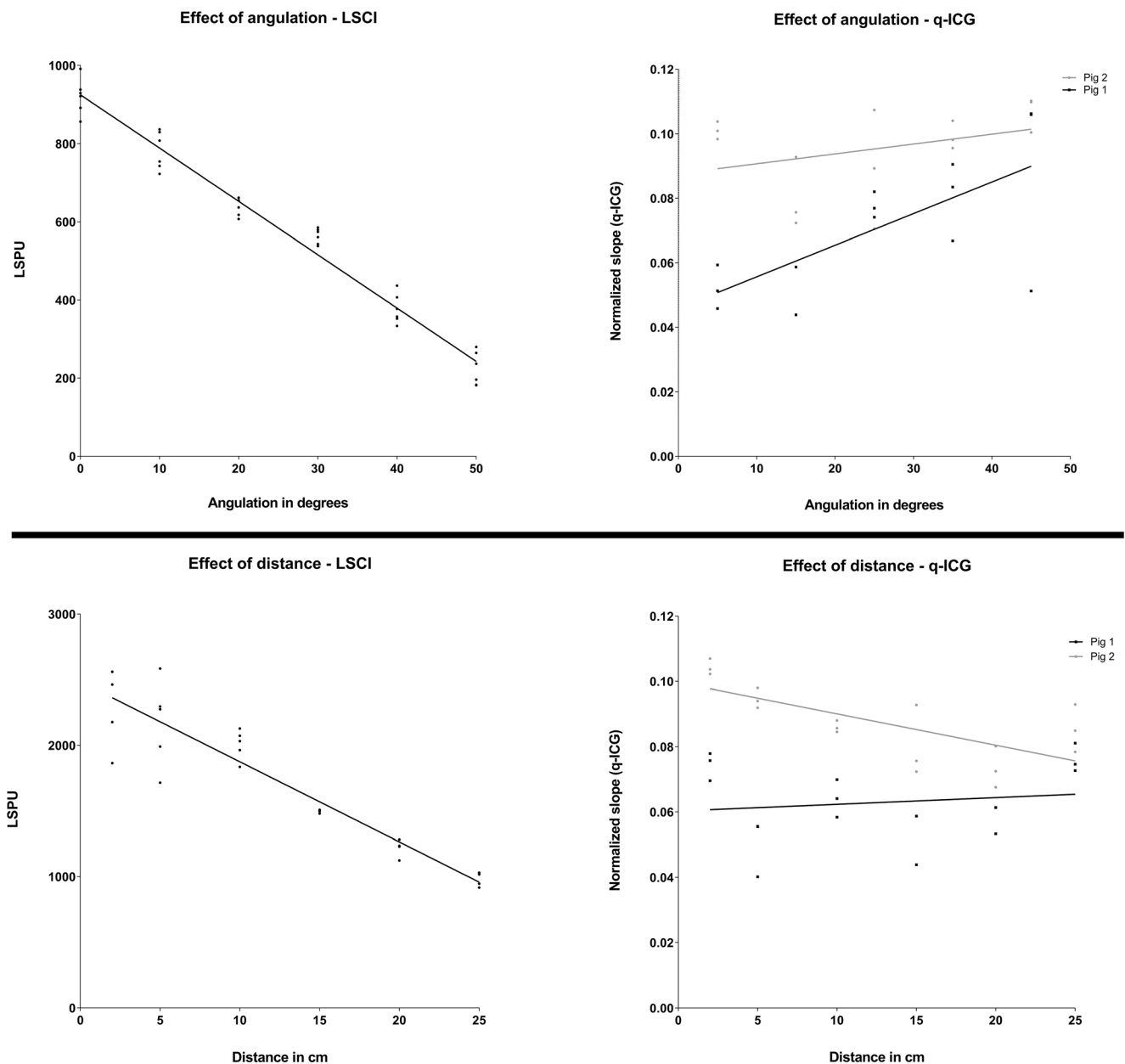


Fig. 6 The effect of altered angulation and distance between measuring device and target surface on measurements obtained by LSCI (flow model, five or six ROIs/measurement) and q-ICG (three ROIs/measurement, $n = 2$ pigs). Note the intrinsic angulation of the ICG scope, see methods. A sharp decrease in LSPU is observed with

increasing angulation and distance, whereas the q-ICG method varies less in obtained values. Normalized slope calculated as $(\Delta \text{fluorescence} / \Delta \text{time}) / (\text{max fluorescence} - \text{baseline fluorescence})$. LSCI laser speckle contrast imaging, q-ICG quantitative indocyanine green, LSPU laser speckle perfusion units

Considering the poor correlation between the two modalities, these results suggest that during experimental conditions, LSCI and q-ICG do not estimate blood flow through tissues similarly. This is possibly due to different penetration depths of measurements as 95 % of the signal that LSCI detects is from the top 700- μm layer of tissue (serosa) [32], whereas q-ICG has been shown to penetrate several millimeters to centimeters (including mucosa) [33].

Investigating the data from de-vascularized intestine and stomach as a percentage of a baseline mean revealed a

concordance between flow assessed by q-ICG and LSCI. When evaluating tissue perfusion in a clinical setting, assessing ischemia in comparison to the normally perfused tissue may be more proper, as absolute values might differ from person to person.

Previous studies have evaluated the correlation between LSCI and q-ICG vs. radioactively labeled microspheres [19, 22, 34]. Microspheres are considered a gold standard for microvascular flow assessment [22, 35–37], and the technique relies on intraaortic or intracardiac injection of microspheres

which are brought into peripheral tissues by the circulation and lodges in peripheral capillaries. Then, by measuring the radioactivity contained within the tissue of interest, the microvascular perfusion can be estimated. Studies have found strong correlations between q-ICG and microsphere assessed perfusion ($r = 0.92\text{--}0.96$, $p < 0.001$) [19, 22]. However, for LSCI and microspheres measured in the stomach tissue, only a moderate correlation could be demonstrated ($r = 0.54$, $p = 0.045$) [Ambrus, unpublished]. Still, the microspheres method represent a snapshot of the tissue perfusion measured in milliliters per minute per gram of tissue, and the perfusion of the full tissue wall is evaluated. In contrast, LSCI perfusion corresponds to a mean flux recorded over the sample time (30 s), and the penetration depth is no more than 700 μM [34].

Considering these observations, q-ICG may be a more sensitive method to detect early ischemic changes [38] due to the deeper tissue penetration compared with LSCI. Consequently, q-ICG may be a more sensitive measure than LSCI for evaluating anastomotic health and viability since mucosal ischemia may occur before transmural progression, i.e., postoperatively. Nevertheless, it is challenging to grade transmural ischemic changes, and in this situation, a combination of LSCI and q-ICG could be useful.

A linear decrease in LSPU was demonstrated when the distance or angulation between the laser head and the target tissue was increased. In open surgery, obtaining a standardized distance and angle to the abdomen is relatively easy, as well as placing intestines in plain view, thus minimizing the impact of distance and angulation. On the other hand, applying LSCI in a minimally invasive setting may prove difficult. From a laparoscopic point of view, ensuring that the target structures are located within the same distance and angle of the camera

could be challenging. Also, no laparoscopic or robot-assisted LSCI-system is currently available on the market.

A systematic review of 14 non-randomized studies including patients undergoing colorectal ($n = 916$) or esophageal resections ($n = 214$) indicated that the use of ICG-FA assisted assessment of perfusion was associated with a lower risk of anastomotic dehiscence [18]. The studies were non-randomized and relied mostly on the visual interpretation of ICG-FA increasing the risk of observer bias. LSCI and q-ICG allow for quantitative assessments of tissue perfusion, and the next step would be to determine a clinically relevant “perfusion threshold” for anastomotic viability. By defining such a threshold, the surgeon has the option to change strategy intraoperatively by, e.g., forming a stoma instead of a primary anastomosis or expanding the resection margin until the tissue is well-perfused [18, 19, 26]. An objective quantitative perfusion assessment could potentially reduce anastomotic dehiscence by being more reliable than a traditional, clinical assessment of anastomotic health [7]. Whether this threshold should be in absolute values or a relative difference to normal tissue is unclear.

Unlike q-ICG, LSCI allows for continuous assessment of perfusion before, during, and after the establishment of an anastomosis, because LSCI only relies on illumination with laser light and no contrast agent is required. Q-ICG is limited by the metabolism of ICG with a plasma half-life of 3 to 5 min [39]. However, some ICG is retained in the tissue, and re-injection of ICG may limit the visual interpretation of the ICG-FA. Though, repeated quantitative evaluation with q-ICG seems possible when the method is slightly modified [40]. When using q-ICG, it is of utmost importance to evaluate perfusion immediately after injection, as the slope (or the

Table 1 Properties of ICG-FA and LSCI

Property of method	LSCI	ICG-FA
Continuous evaluation	Possible	Limited by ICG metabolism
Influenced by the distance to the tissue	Highly, but linear	Minimally
Influenced by observation angle	Highly, but linear	Minimally
Laparoscopy	Currently not possible	Possible
Robot-assisted surgery	Currently not possible	Possible
Contrast agent	No	Yes
Depth of penetration	Up to 1 mm through tissue	Several mm to 2 cm
Other properties than perfusion assessment	No	Cholangiography [42] Identification of [42]: Tumors Metastases Lymph nodes/vessels Ureter
Adverse effects	None reported	Extremely rare [11]
Allergy	None reported	Extremely rare [11]

ICG-FA indocyanine green fluorescence angiography, LSCI laser speckle contrast imaging, ICG indocyanine green

time-to-peak) is calculated from the fluorescence time curve of the first pass through the region of interest [19, 41]. Besides assessment of tissue perfusion and visualization of the microvasculature, ICG-FA may visualize biliary structures, and differentiate lymph nodes and tumors from healthy tissue [42], whereas LSCI has currently no other clinical utilities. For a quick overview of the different properties of LSCI and q-ICG, please consult Table 1.

The present study has certain strengths and limitations. Data were obtained during standardized and controlled conditions, and significant correlations were found. The porcine model was based on a well-established model of intestinal ischemia. The use of a phantom flow model allows for complete control of infusion rates and offers good control of environmental factors which could affect the measurements. However, the flow models are not representative of biological tissues as it only consisted of a single tube, while the signal will be derived from a vast capillary network when measuring on the serosal side of the intestine. Also, the caval vein model only represented venous flow, and further studies should address the validation on arterial vessels and mucosal surfaces. Another limitation was the use of two different flow models which may limit the comparability of differences in angulation and distance. The flow models were different in flow rates and velocity, as the *ex vivo* model had a flow rate of 9.5 ml/min and velocity of 24.7 cm/min. This is far less than the flow and velocity in the porcine inferior caval vein (900–1400 ml/min) [43, 44]. However, as no comparisons were made between the models and methods, we accept these differences to illustrate the impact of angulation and distance on perfusion measures.

Regarding the assessment of de-vascularized bowel segments, it should be mentioned that measurements were done after 30 min where ischemia might often be macroscopically visible. However, this study was not designed to investigate the sensibility or specificity of q-ICG/LSCI in discriminating normal from ischemic tissue; further studies should investigate this issue.

Conclusion

The overall correlation between q-ICG and LSCI for the assessment of intestinal perfusion was low, indicating that the modalities cannot be used interchangeably, but may supplement each other as each modality has its limitations and strengths. A combination of the methods may show the extent of ischemic changes in tissue. LSCI is profoundly affected by angulation and distance. In comparison, q-ICG is minimally affected by changing experimental conditions and is more readily applicable in minimally invasive surgery.

Acknowledgments The study was sponsored by donations from private foundations, to whom the authors owe gratitude: Mogens Andresen fonden, Civilingeniør Johannes Elmqvist Ormstrup og Hustru Grete Ormstrups Fond, and Fabrikant Frands Køhler Niensens og Hustrus Mindelegat. Sponsors had no role in study design, interpretation of results, or any other part of the study. Also, a sincere thanks to Jens Osterkamp, MD, for the help with illustrations.

Authors' contributions Study conception and design: JHR, NN, LBS, MPA. Acquisition of data: JHR, RA, NN, RBS. Analysis and interpretation of data: JHR, NN, RBS, MBS, RA, LBS, MPA. Drafting of the manuscript: JHR, NN. Critical revision and final approval of the manuscript: JHR, NN, RBS, MBS, RA, LBS, MPA.

Compliance with ethical standards

Conflict of interest The authors declare that they have no conflict of interest.

Ethical approval All applicable international, national, and institutional guidelines for the care and use of animals were followed. All procedures performed in studies involving animals were in accordance with the ethical standards of the institution or practice at which the studies were conducted.

Abbreviations ICG, Indocyanine green; ICG-FA, Indocyanine green-fluorescence angiography; LSCI, Laser speckle contrast imaging; LSPU, Laser speckle perfusion units; q-ICG, Quantitative indocyanine green fluorescence angiography; ROI, Region of interest; RPM, Revolutions per minute

References

1. Thompson SK, Chang EY, Jobe BA (2006) Clinical review: healing in gastrointestinal anastomoses, part I. *Microsurgery* 26:131–136. <https://doi.org/10.1002/micr.20197>
2. Chadi SA, Fingerhut A, Berho M, DeMeester SR, Fleshman JW, Hyman NH, Margolin DA, Martz JE, McLemore EC, Molena D, Newman MI, Rafferty JF, Safar B, Senagore AJ, Zmora O, Wexner SD (2016) Emerging trends in the etiology, prevention, and treatment of gastrointestinal anastomotic leakage. *J Gastrointest Surg* 20:2035–2051. <https://doi.org/10.1007/s11605-016-3255-3>
3. Vignali A, Gianotti L, Braga M, Radaelli G, Malvezzi L, Di Carlo V (2000) Altered microperfusion at the rectal stump is predictive for rectal anastomotic leak. *Dis Colon Rectum* 43:76–82
4. Kofoed SC, Calatayud D, Jensen LS, Helgstrand F, Achiam MP, De Heer P, Svendsen LB (2015) Intrathoracic anastomotic leakage after gastroesophageal cancer resection is associated with increased risk of recurrence. *J Thorac Cardiovasc Surg* 150:42–48. <https://doi.org/10.1016/j.jtcvs.2015.04.030>
5. Kofoed SC, Calatayud D, Jensen LS, Jensen MV, Svendsen LB (2014) Intrathoracic anastomotic leakage after gastroesophageal cancer resection is associated with reduced long-term survival. *World J Surg* 38:114–119. <https://doi.org/10.1007/s00268-013-2245-9>
6. Karliczek A, Benaron DA, Baas PC, Zeebregts CJ, Wiggers T, van Dam GM (2010) Intraoperative assessment of microperfusion with visible light spectroscopy for prediction of anastomotic leakage in colorectal anastomoses. *Colorectal disease: the official journal of the Association of Coloproctology G B Irel* 12:1018–1025. <https://doi.org/10.1111/j.1463-1318.2009.01944.x>

7. Karliczek A, Harlaar NJ, Zeebregts CJ, Wiggers T, Baas PC, van Dam GM (2009) Surgeons lack predictive accuracy for anastomotic leakage in gastrointestinal surgery. *Int J Color Dis* 24:569–576. <https://doi.org/10.1007/s00384-009-0658-6>
8. Mimezami A, Mirnezami R, Chandrakumaran K, Sasapu K, Sagar P, Finan P (2011) Increased local recurrence and reduced survival from colorectal cancer following anastomotic leak: systematic review and meta-analysis. *Ann Surg* 253:890–899. <https://doi.org/10.1097/SLA.0b013e3182128929>
9. Jessen M, Nerstrom M, Wilbek TE, Roepstorff S, Rasmussen MS, Krarup PM (2016) Risk factors for clinical anastomotic leakage after right hemicolectomy. *Int J Color Dis* 31:1619–1624. <https://doi.org/10.1007/s00384-016-2623-5>
10. Briers JD, Fercher AF (1982) Retinal blood-flow visualization by means of laser speckle photography. *Invest Ophthalmol Vis Sci* 22:255–259
11. Owens SL (1996) Indocyanine green angiography. *Br J Ophthalmol* 80:263–266
12. Yannuzzi LA, Slakter JS, Sorenson JA, Guyer DR, Orlock DA (2012) Digital indocyanine green videoangiography and choroidal neovascularization. 1992. *Retina* 32(Suppl 1):191
13. Valdes PA, Roberts DW, Lu FK, Golby A (2016) Optical technologies for intraoperative neurosurgical guidance. *Neurosurg Focus* 40:E8. <https://doi.org/10.3171/2015.12.focus15550>
14. Fredrickson VL, Russin JJ, Strickland BA, Bakhsheshian J, Amar AP (2017) Intraoperative imaging for vascular lesions. *Neurosurg Clin N Am* 28:603–613. <https://doi.org/10.1016/j.nec.2017.05.011>
15. Kaiser M, Yafi A, Cinat M, Choi B, Durkin AJ (2011) Noninvasive assessment of burn wound severity using optical technology: a review of current and future modalities. *Burns* 37:377–386. <https://doi.org/10.1016/j.burns.2010.11.012>
16. Alander JT, Kaartinen I, Laakso A, Patila T, Spillmann T, Tuchin VV, Venermo M, Valisuo P (2012) A review of indocyanine green fluorescent imaging in surgery. *Int J Biomed Imaging* 2012:940585. <https://doi.org/10.1155/2012/940585>
17. Marano A, Priora F, Lenti LM, Ravazzoni F, Quarati R, Spinoglio G (2013) Application of fluorescence in robotic general surgery: review of the literature and state of the art. *World J Surg* 37:2800–2811. <https://doi.org/10.1007/s00268-013-2066-x>
18. Degett TH, Andersen HS, Gogenur I (2016) Indocyanine green fluorescence angiography for intraoperative assessment of gastrointestinal anastomotic perfusion: a systematic review of clinical trials. *Langenbeck's Arch Surg* 401:767–775. <https://doi.org/10.1007/s00423-016-1400-9>
19. Nerup N, Andersen HS, Ambrus R, Strandby RB, Svendsen MBS, Madsen MH, Svendsen LB, Achiam MP (2017) Quantification of fluorescence angiography in a porcine model. *Langenbeck's Arch Surg* 402:655–662. <https://doi.org/10.1007/s00423-016-1531-z>
20. Diana M, Agnus V, Halvax P, Liu YY, Dallemagne B, Schlagowski AI, Geny B, Diemunsch P, Lindner V, Marescaux J (2015) Intraoperative fluorescence-based enhanced reality laparoscopic real-time imaging to assess bowel perfusion at the anastomotic site in an experimental model. *Br J Surg* 102:e169–e176. <https://doi.org/10.1002/bjs.9725>
21. Wada T, Kawada K, Takahashi R, Yoshitomi M, Hida K, Hasegawa S, Sakai Y (2017) ICG fluorescence imaging for quantitative evaluation of colonic perfusion in laparoscopic colorectal surgery. *Surg Endosc* 31:4184–4193. <https://doi.org/10.1007/s00464-017-5475-3>
22. Toens C, Krones CJ, Blum U, Fernandez V, Grommes J, Hoelzl F, Stumpf M, Klinge U, Schumpelick V (2006) Validation of IC-VIEW fluorescence videography in a rabbit model of mesenteric ischaemia and reperfusion. *Int J Color Dis* 21:332–338. <https://doi.org/10.1007/s00384-005-0017-1>
23. Nadort A, Kalkman K, van Leeuwen TG, Faber DJ (2016) Quantitative blood flow velocity imaging using laser speckle flowmetry. *Sci Rep* 6:25258. <https://doi.org/10.1038/srep25258>
24. Forrester KR, Tulip J, Leonard C, Stewart C, Bray RC (2004) A laser speckle imaging technique for measuring tissue perfusion. *IEEE Trans Biomed Eng* 51:2074–2084. <https://doi.org/10.1109/TBME.2004.834259>
25. Senarathna J, Rege A, Li N, Thakor NV (2013) Laser speckle contrast imaging: theory, instrumentation and applications. *IEEE Rev Biomed Eng* 6:99–110. <https://doi.org/10.1109/RBME.2013.2243140>
26. Ambrus R, Strandby RB, Svendsen LB, Achiam MP, Steffensen JF, Sondergaard Svendsen MB (2016) Laser speckle contrast imaging for monitoring changes in microvascular blood flow. *Eur Surg Res* 56:87–96. <https://doi.org/10.1159/000442790>
27. Kilkenny C, Browne WJ, Cuthill IC, Emerson M, Altman DG (2010) Improving bioscience research reporting: the ARRIVE guidelines for reporting animal research. *PLoS Biol* 8:e1000412. <https://doi.org/10.1371/journal.pbio.1000412>
28. Diana M, Noll E, Diemunsch P, Dallemagne B, Benahmed MA, Agnus V, Soler L, Barry B, Namer IJ, Demartines N, Charles AL, Geny B, Marescaux J (2014) Enhanced-reality video fluorescence: a real-time assessment of intestinal viability. *Ann Surg* 259:700–707. <https://doi.org/10.1097/SLA.0b013e31828d4ab3>
29. Mukaka MM (2012) Statistics corner: a guide to appropriate use of correlation coefficient in medical research. *Malawi Med J* 24:69–71
30. Lee IA, Preacher KJ (2013) Calculation for the test of the difference between two dependent correlations with one variable in common [Computer software]. Available from <http://quantpsy.org>. Accessed 11 Jan 2018
31. Steiger JH (1980) Tests for comparing elements of a correlation matrix. *Psychol Bull* 87:245–251. <https://doi.org/10.1037/0033-2909.87.2.245>
32. Davis MA, Kazmi SM, Dunn AK (2014) Imaging depth and multiple scattering in laser speckle contrast imaging. *J Biomed Opt* 19:086001. <https://doi.org/10.1117/1.jbo.19.8.086001>
33. Frangioni JV (2008) New technologies for human cancer imaging. *J Clin Oncol* 26:4012–4021. <https://doi.org/10.1200/jco.2007.14.3065>
34. Ambrus R, Strandby RB, Secher NH, Runitz K, Svendsen MB, Petersen LG, Achiam MP, Svendsen LB (2016) Thoracic epidural analgesia reduces gastric microcirculation in the pig. *BMC Anesthesiol* 16:86. <https://doi.org/10.1186/s12871-016-0256-4>
35. Heymann MA, Payne BD, Hoffman JJ, Rudolph AM (1977) Blood flow measurements with radionuclide-labeled particles. *Prog Cardiovasc Dis* 20:55–79
36. Lange M, Hamahata A, Traber DL, Nakano Y, Traber LD, Enkhbaatar P (2013) Multiple versus single injections of fluorescent microspheres for the determination of regional organ blood flow in septic sheep. *Lab Anim* 47:203–209. <https://doi.org/10.1177/0023677213487718>
37. Reinhardt CP, Dalhberg S, Tries MA, Marcel R, Leppo JA (2001) Stable labeled microspheres to measure perfusion: validation of a neutron activation assay technique. *Am J Physiol Heart Circ Physiol* 280:H108–H116
38. Alemanno G, Somigli R, Prosperi P, Bergamini C, Maltinti G, Giordano A, Valeri A (2016) Combination of diagnostic laparoscopy and intraoperative indocyanine green fluorescence angiography for the early detection of intestinal ischemia not detectable at CT scan. *Int J Surg Case Rep* 26:77–80. <https://doi.org/10.1016/j.ijscr.2016.07.016>
39. Shimizu S, Kamiike W, Hatanaka N, Yoshida Y, Tagawa K, Miyata M, Matsuda H (1995) New method for measuring ICG Rmax with a clearance meter. *World J Surg* 19:113–118 discussion 118
40. Nerup N, Knudsen KBK, Ambrus R, Svendsen MBS, Thymann T, Ifaoui IBR, Svendsen LB, Achiam MP (2017) Reproducibility and reliability of repeated quantitative fluorescence angiography. *Surg Technol Int* 31:35–39

41. Quero G, Lapergola A, Barberio M, Seeliger B, Saccomandi P, Guerriero L, Mutter D, Saadi A, Worreth M, Marescaux J, Agnus V, Diana M (2018) Discrimination between arterial and venous bowel ischemia by computer-assisted analysis of the fluorescent signal. *Surg Endosc*. <https://doi.org/10.1007/s00464-018-6512-6>
42. Baiocchi GL, Diana M, Boni L (2018) Indocyanine green-based fluorescence imaging in visceral and hepatobiliary and pancreatic surgery: state of the art and future directions. *World J Gastroenterol* 24:2921–2930. <https://doi.org/10.3748/wjg.v24.i27.2921>
43. Ortega AE, Richman MF, Hernandez M, Peters JH, Anthonie GJ, Azen S, Beart RW Jr (1996) Inferior vena caval blood flow and cardiac hemodynamics during carbon dioxide pneumoperitoneum. *Surg Endosc* 10:920–924
44. Lindberg F, Bergqvist D, Rasmussen I, Haglund U (1997) Hemodynamic changes in the inferior caval vein during pneumoperitoneum. An experimental study in pigs. *Surg Endosc* 11:431–437

Publisher's note Springer Nature remains neutral with regard to jurisdictional claims in published maps and institutional affiliations.